Adipocyte-Specific Modulation of KLF14 Expression in Mice Leads to Sex-Dependent Impacts on Adiposity and Lipid Metabolism

Qianyi Yang,[1] Jameson Hinkle,[1] Jordan N. Reed,[1,2] Redouane Aherrahrou,[1] Zhiwen Xu,[3] Thurl E. Harris,[4] Erin J. Stephenson,[5] Kiran Musunuru,[6,7,8] Susanna R. Keller,[9] and Mete Civelek[1,2]

Diabetes 2022;71:677–693 | https://doi.org/10.2337/db21-0674

Genome-wide association studies identified single nucleotide polymorphisms on chromosome 7 upstream of *KLF14* to be associated with metabolic syndrome traits and increased risk for type 2 diabetes (T2D). The associations were more significant in women than in men. The risk allele carriers expressed lower levels of the transcription factor KLF14 in adipose tissues than nonrisk allele carriers. To investigate how adipocyte KLF14 regulates metabolic traits in a sex-dependent manner, we characterized high-fat diet–fed male and female mice with adipocyte-specific *Klf14* deletion or overexpression. *Klf14* deletion resulted in increased fat mass in female mice and decreased fat mass in male mice. Female *Klf14*-deficient mice had overall smaller adipocytes in subcutaneous fat depots but larger adipocytes in parametrial depots, indicating a shift in lipid storage from subcutaneous to visceral fat depots. They had reduced metabolic rates and increased respiratory exchange ratios consistent with increased use of carbohydrates as an energy source. Fasting- and isoproterenol-induced adipocyte lipolysis was defective in female *Klf14*-deficient mice, and concomitantly, adipocyte triglycerides lipase mRNA levels were downregulated. Female *Klf14*-deficient mice cleared blood triglyceride and nonesterified fatty acid less efficiently than wild-type. Finally, adipocyte-specific overexpression of *Klf14* resulted in lower total body fat in female but not male mice. Taken together, consistent with human studies, adipocyte KLF14 deficiency in female but not in male mice causes increased adiposity and redistribution of lipid storage from subcutaneous to visceral adipose tissues. Increasing KLF14 abundance in adipocytes of females with obesity and T2D may provide a novel treatment option to alleviate metabolic abnormalities.

Genome-wide association studies (GWAS) identified several genetic variants on chromosome 7 upstream of the *KLF14* gene to be associated with a multitude of metabolic abnormalities, including insulin resistance, type 2 diabetes (T2D), and coronary artery disease (1–4). The associations were more pronounced in women than in men (5). GWAS of gene expression performed in the Multiple Tissue Human Expression Resource (MuTHER) and the Metabolic Syndrome in Men (METSIM) cohorts identified the maternally imprinted *KLF14* gene as a master regulator of gene expression in subcutaneous adipose tissue only, although KLF14 is expressed at low levels across most human tissues (6–9). GWAS-associated single

[1]Center for Public Health Genomics, School of Medicine, University of Virginia, Charlottesville, VA
[2]Department of Biomedical Engineering, School of Engineering and Applied Science, University of Virginia, Charlottesville, VA
[3]Department of Chemistry, College of Arts and Sciences, University of Virginia, Charlottesville, VA
[4]Department of Pharmacology, School of Medicine, University of Virginia, Charlottesville, VA
[5]Department of Anatomy, College of Graduate Studies & Chicago College of Osteopathic Medicine, Midwestern University, Downers Grove, IL
[6]Cardiovascular Institute, Perelman School of Medicine at the University of Pennsylvania, Philadelphia, PA
[7]Division of Cardiovascular Medicine, Department of Medicine, Perelman School of Medicine at the University of Pennsylvania, Philadelphia, PA
[8]Department of Genetics, Perelman School of Medicine at the University of Pennsylvania, Philadelphia, PA
[9]Division of Endocrinology and Metabolism, Department of Medicine, School of Medicine, University of Virginia, Charlottesville, VA

Corresponding authors: Qianyi Yang, qy5sy@virginia.edu, and Mete Civelek, mete@virginia.edu

Received 28 July 2021 and accepted 17 January 2022

This article contains supplementary material online at https://doi.org/10.2337/figshare.18631502.

nucleotide polymorphisms (SNPs) were also associated with KLF14 expression levels in *cis* and nearly 400 genes in *trans* in adipose tissue (1,6,10). The locus is one of the largest *trans*-expression quantitative trait loci hotspots known in the human genome (7). The results suggested that disease-associated variants act in adipose tissue to increase disease risk. However, given that adipose tissue contains a multitude of cell types, it was not clear which cells were ultimately responsible for KLF14's adverse effects.

Several studies have implicated KLF14, a single-exon gene in the Krüppel-like factor family of transcription factors, in the development of metabolic diseases, including obesity, insulin resistance, and T2D. Small et al. (1) demonstrated that lowering KLF14 expression in preadipocytes from females prevented maturation to adipocytes, as measured by the expression of adipogenesis markers and lipid accumulation. Histological analysis of subcutaneous adipose tissue biopsy specimens showed that females who were homozygous for the T2D risk allele had larger adipocytes, suggesting that lower KLF14 expression is associated with adipocyte dysfunction (1). Collectively, these studies implied that KLF14 plays roles in adipogenesis and mature adipocyte size and function. T2D-associated variants also have strong associations with HDL and triglyceride (TG) levels in the serum (11,12). However, the mechanisms by which KLF14 regulates adipocyte differentiation and function are not known.

To further investigate the role of KLF14 in adipocytes and to establish a mouse model that is relevant to humans, we characterized mice with adipocyte-specific *Klf14* deletion or overexpression. Our findings demonstrate that adipocyte KLF14 is a key regulator of lipid metabolism and consistent with findings that this regulation is female-specific in humans. Our findings may facilitate the development of novel therapeutics to treat obesity and related metabolic diseases specifically in females.

RESEARCH DESIGN AND METHODS

Generation of Mice With Adipocyte-Specific Deletion and Overexpression of *Klf14*

The generation of adipocyte-specific *Klf14*-knockout (KO) mice has been described in detail elsewhere (1). Briefly, in vitro transcribed Cas9 mRNA, two guide RNAs designed to target sites upstream and downstream of the *Klf14* gene locus, two single-strand DNA oligonucleotides bearing loxP sequences, along with 80-nt homology arms matching the target sites, were injected into the cytoplasm of fertilized oocytes from C57BL/6J mice (Supplementary Fig. 1*A*). Genomic DNA samples from founders were screened for correct loxP sequences flanking the *Klf14* gene by PCR and confirmed by Sanger sequencing. Mice with two loxP sites that segregated on the same chromosome were bred with *Adipoq*-Cre mice on the C57BL/6J background (B6; FVB-Tg [*Adipoq*-Cre]1Evdr/J, The Jackson Laboratory) to obtain litters with homozygous *Klf14* loxP knock-in mice that were Cre^+ ($Klf14^{fl/fl}$*Adipoq*-Cre^+ or KO) and wild-type (WT) mice that were positive for *Klf14* loxP but negative for *Adipoq*-Cre ($Klf14^{fl/fl}$*Adipoq*-Cre^- or WT) for experiments. The presence of the *Adipoq*-Cre allele was confirmed by PCR (Supplementary Table 1). Absence of KLF14 protein expression in adipocytes isolated from KO animals was confirmed by Western blotting (Supplementary Fig. 1*B*). To generate mice with adipocyte-specific overexpression of *Klf14*, *Klf14* was PCR amplified from C57BL/6J cDNA and cloned downstream of the 5.43 kilobase (kb) adiponectin (*Adipoq*) promoter at an *Eco*RV site using Gibson Assembly into the pADNpcDNA3.1 KanR vector. The 8.2-kb expression cassette containing the *Adipoq* promoter, *Klf14* cDNA, and 3′ untranslated region was gel purified after restriction digestion with *Not*I and NgoMIV. The transgene was injected into pronuclei of fertilized C57BL/6N eggs to produce random integrants at the University of California, Irvine Transgenic Mouse Facility. The presence of the transgene was confirmed by PCR (primers are listed in Supplementary Table 1). We labeled these mice *Adipoq-Klf14*-OE. Increased KLF14 protein expression in adipocytes isolated from transgenic animals was confirmed by Western blotting (Supplementary Fig. 1*C*).

Animal Husbandry

All animal protocols were approved by the University of Virginia Animal Care and Use Committee. Mice were maintained in a 12-h light/12-h dark cycle with free access to water and standard chow (Envigo Teklad LM-485 irradiated mouse/rat sterilizable diet, Cat No. 7912). For high-fat diet (HFD) studies, the mice were fed a rodent diet with 40% kcal fat, 43% kcal carbohydrate, and 17% kcal protein (Research Diets, Cat No. D12079B). The mice were euthanized by cervical dislocation after induction of deep anesthesia using isoflurane, consistent with the recommendations of the Panel of the American Veterinary Medical Association.

Body Composition Analysis

Total body fat and lean mass were assessed in conscious mice using a noninvasive quantitative MRI system (Echo Medical Systems, Cat No. EchoMRI 3-in-1 v2.1), as previously reported (13).

Glucose and Insulin Tolerance Tests

Glucose and insulin tolerance tests were performed as previously described (14). For the glucose tolerance test, mice were fasted from 7 A.M. to 1 P.M. and were administered glucose at 1 mg/g body weight intraperitoneally. Blood glucose levels were measured with a OneTouch Ultra Glucometer (LifeScan) in blood drops obtained from nicked tail veins before and at 10, 20, 30, 60, 90, and 120 min after the injection. The insulin tolerance test was performed at 1–2 P.M. on mice fed ad libitum. Insulin (100 units/mL; Humulin, Eli Lilly) at 0.75 units/kg body weight was administered by

intraperitoneal injection of 0.25 units/mL solution in 0.9% NaCl. Blood glucose levels were measured immediately before and at 15, 30, 45, 60, and 90 min after the injection.

Plasma Insulin and Lipid Analysis

Mice were either fed ad libitum, and samples taken between 7 A.M. and 8 A.M., or they were fasted for 6 h from 7 A.M. to 1 P.M. before samples were taken. Whether measurements were done in the fed or fasted state is indicated in the *Results* section. For insulin, fatty acids, and glycerol measurements, blood samples were collected through retro-orbital bleeding or cardiac puncture. For HDL, total cholesterol, and TG measurements, plasma was obtained using heparinized capillary tubes, followed by centrifugation at 7,800 relative centrifugal force in a microfuge for 10 min at 4°C. Insulin levels were measured with an ELISA (Alpco, Cat No. 80-INSMSU-E01). Total cholesterol, HDL, and TG levels were measured using colorimetric assays (FUJIFILM Wako Diagnostics, Cat Nos. 999-02601, 997-72591, 464-01601).

Indirect Calorimetry Analysis

For determination of energy expenditure and respiratory exchange ratios (RERs), mice were placed in Oxymax metabolic chambers (Comprehensive Laboratory Animal Monitoring System [CLAMS] from Columbus Instruments), under a constant environmental temperature (22°C) and a 12-h light, 12-h dark cycle, as previously described (15). V_{O_2}, V_{CO_2}, and ambulatory activity were determined for each mouse every 5 min over a 72-h period. Experimental mice were acclimated to the cages during the first 24 h. Measurements taken during the following 48 h were used for data analysis. RERs were calculated as V_{CO_2}/V_{O_2}. Carbohydrate use was calculated as (20 kJ/L × V_{O_2} uptake) × [(RER − 0.7)/0.3], and fat use was calculated as (20 kJ/L × V_{O_2} uptake) × (1 − [(RER × 0.7)/0.3)] (16). Both body fat and lean mass were included as covariates in the models used to analyze data obtained from the CLAMS experiments. Mice in each chamber had free access to water and food. Locomotor activity was monitored by a multidimensional infrared light beam system surrounding each cage.

In Vivo Lipolysis

To determine lipolysis in vivo, two different experiments were performed. For lipolysis under fasting condition, blood samples were drawn from tail veins of 24-week-old mice using nonheparinized glass capillary tubes at 5 P.M. before food was withdrawn and at 9 A.M. after 16-h fasting to measure nonesterified fatty acids (NEFAs) and glycerol. For β-adrenergic receptor stimulation experiments, blood samples were drawn from tail veins of random-fed 25-week-old mice via nonheparinized glass capillary tubes before stimulation. After a short recovery period (30 min), mice were injected intraperitoneally with 10 mg/kg isoproterenol (prepared in saline; Sigma-Aldrich, Cat No. I6504). A second blood sample was collected 15 min post-injection. Blood from nonheparinized capillary tubes was allowed to clot on ice before centrifugation at 500*g* for 20 min at 4°C. Glycerol and NEFA concentrations in serum were determined colorimetrically using commercially available reagents (Sigma-Aldrich, Cat No. F6428; Wako Life Sciences, Cat No. NEFA-HR [2]).

Ex Vivo Lipolysis

Isolated mature adipocytes were diluted in DMEM/F12 with 2.5% BSA to a concentration of 0.5 million cells/mL, and 200 μL with 100,000 cells was used for each reaction. To induce lipolysis, 30 μmol/L isoproterenol was added to diluted adipocytes, followed by incubation at 37°C with shaking at 150 rpm. After incubation, infranatant was removed to a new tube, and NEFA measurements were performed (Wako Life Sciences, Cat No. NEFA-HR [2]).

In Vivo Lipid Challenge

Experimental mice were fasted for 4 h before the test (7–11 A.M.). Olive oil (6 μL/g body weight) was given by oral gavage, as described previously (17). Blood samples were drawn via heparinized (for TG)/nonheparinized (for NEFA) capillary tubes from tail veins before (time 0) and at 1, 2, 3, and 4 h after gavage. TG and NEFA measurements were performed as described above.

Determination of Adipocyte Sizes

Subcutaneous white adipose tissue (sWAT) and parametrial-periovarian/epididymal (pWAT/eWAT) from four mice of each sex and genotype was excised and fixed in 10% neutral buffered formalin (18). Tissues were embedded in paraffin, and 5-μm-thick sections were prepared and stained with hematoxylin and eosin at the University of Virginia Research Histology Core. Slides were scanned, and images were acquired with an EVOS microscope camera. Quantification of adipocyte size was done using ImageJ 1.48 (19). Images were processed as described previously (20).

Sex Hormone Measurements

Mouse sera collected at the time of euthanasia were stored at −80°C. After thawing, they were allowed to equilibrate at room temperature and spun to remove aggregates. Then, 100 μL of 1:10 diluted sera per well were aliquoted for ELISA in 96-well plates. Free testosterone, progesterone, and estradiol levels were measured using the Testosterone Parameter assay kit (R&D Systems, Cat No. KGE010), Progesterone ELISA Kit (Cayman Chemical, Cat No. 582601), and Estradiol ELISA Kit (Cayman Chemical, Cat No. 501890), following the manufacturers' instructions (21).

Primary Mouse Adipocyte Isolation

Adipocytes were isolated from sWAT and pWAT/eWAT, as previously described (22). Immediately after euthanization, fat pads were removed, placed in Krebs Ringer HEPES (KRH)–BSA buffer containing collagenase type I (1 mg/mL, 2 mg/g of tissue; Worthington Biochemical Corp.) and minced with scissors. Small tissue pieces were incubated in a 37°C shaking water bath (100 rpm) for 1 h. Fat cells were separated from nonfat cells and undigested debris by filtration through a 0.4-mm Nitex nylon mesh (Tetko) and four washes by flotation with KRH buffer without BSA. After centrifugation at 1,000*g* for 15 min at 4°C, the isolated fat cells floating on the surface were used for total RNA extraction and preparation of cell lysates for immunoblotting.

Total RNA Extraction, cDNA Synthesis and Real-Time PCR

Total RNA was isolated from parametrial-periovarian/epididymal and subcutaneous adipocytes using a combination of TRIzol Reagent (Thermo Fisher Scientific, Waltham, MA) and miRNeasy kit (Qiagen, Hilden, Germany) according to the manufacturers' instructions (23). Adipocytes isolated from 200 mg of tissue in the previous step were homogenized in 2 mL of TRIzol Reagent using the Tissue-Tearor homogenizer (Model 985370, BioSpec Products). After homogenization, samples were incubated at room temperature for 5 min and centrifuged at 12,000*g* for 10 min at 4°C. The resulting fat monolayer on top was carefully avoided when pipetting the rest of the sample into a clean tube. Then, 400 μL of chloroform was added, and samples were mixed by vortexing. Samples were kept at room temperature for 3 min before centrifugation at 12,000*g* for 30 min at 4°C. After centrifugation, samples separated into three phases with the RNA in the upper phase. The RNA phase was transferred to a new tube without disturbing the interphase. Sample volumes were measured and 1.5× sample volumes of 100% ethanol added. Samples were mixed thoroughly by inverting tubes several times. Samples were then loaded on miRNeasy spin columns (Qiagen), and the manufacturer's protocol was followed for subsequent steps. Total RNA concentrations were quantified using a Qubit Fluorometer and a Qubit RNA BR assay kit (Thermo Fisher Scientific). Then, 1 μg of total RNA was reverse transcribed using SuperScript IV reverse transcriptase (Invitrogen). Real-time PCR was performed in the QuantStudio 5 Real-Time PCR System (Thermo Fisher Scientific) using SYBR Green Master Mix (Roche) and gene-specific primers (Supplementary Table 2).

Cell Culture and Transfection

HEK293 cell line was from ATCC (Manassas, VA) and cultured in DMEM with 10% FBS (Hyclone), 1% L-glutamine, 100 units/mL penicillin, and 100 mg/mL streptomycin at 37°C and 5% CO_2. The pCMV-KLF14-3×FLAG and pCMV-ESR1-HA vectors were purchased from GeneCopoeia (Cat No. EX-I2219-M12 and EX-A0322-M06). These two constructs were transfected into HEK293 cells using Lipofectamine 3000 (Invitrogen) according to the manufacturer's instructions. Stable cell lines were selected with G418 at 500 μg/mL.

Protein Extraction, Immunoblotting, and Immunoprecipitation

Total protein was extracted from cells or tissues using cell lysis buffer (Cell Signaling, Cat No. 9803), containing 20 mmol/L Tris-HCl (pH 7.5), 150 mmol/L NaCl, 1 mmol/L Na_2EDTA, 1 mmol/L EGTA, 1% Triton, 2.5 mmol/L sodium pyrophosphate, 1 mmol/L β-glycerophosphate, 1 mmol/L Na_3VO_4, and 1 μg/mL leupeptin. Protease inhibitor cocktail (Thermo Fisher Scientific) and phosphatase inhibitor (Thermo Fisher Scientific) were added to the lysis buffer before extraction. Protein concentrations were determined using a Pierce BCA Protein Assay Reagent (Pierce Biotechnology). Proteins (10 μg protein/lane) were separated by SDS-PAGE. Electrophoresis was conducted using a XCell II Mini-Cell with 4–12% NuPAGE Tris-acetate gradient SDS-polyacrylamide gels (Invitrogen). Protein samples were transferred onto polyvinylidene difluoride membranes using an XCell II Blot Module (Invitrogen). The membranes were blocked in Intercept (TBS) Blocking Buffer (LI-COR) for 1 h at room temperature, and probed with primary antibody in 0.1% Tween LI-COR blocking buffer overnight at 4°C. The KLF14 antibody was a gift from Dr. Roger D. Cox (MRC Harwell Institute). It was generated at Eurogentec by immunizing rabbits against the C-DMIEYRGRRRTPRIDP-N peptide. Full-length purified KLF14 purchased from Creative BioMart (Cat No. KLF14-481H) served as a positive control. The β-actin antibody was from Cell Signaling Technology (Cat No. 3700s). For measuring hormone-sensitive lipase (HSL) phosphorylation, the antibodies used were phosphorylated (p)HSL (Ser660) antibody and HSL antibody (Cell Signaling Technology, Cat No. 4126S and 4107S). The membranes were washed three times for 10 min each in Tris-buffered saline–0.1% Tween buffer solution and then probed with IRDye-labeled secondary antibodies (926-32211 and 926-68072) in 0.1% Tween LI-COR blocking buffer for 1 h at room temperature. Several washes in Tris-buffered saline–0.1% Tween buffer solution were repeated after labeling with secondary antibodies. The blots were scanned using the LI-COR laser-based image detection method. For immunoprecipitation, cell lysate was incubated with Anti-FLAG M2 Magnetic Beads (MilliporeSigma Cat No. M8823) following the manufacturer's instruction. The associated proteins were analyzed by immunoblotting using estrogen receptor-α antibody (Santa Cruz Biotechnology, Cat No. sc-8002), HA antibody (Abcam, Cat No. ab9110), FLAG M2 antibody (MilliporeSigma, Cat No. F1804), and KLF14 antibody described above.

Statistical Analysis

Trial experiments were used to determine sample size with adequate statistical power. Since the scatter of the data follows normal distribution, all analyses were conducted with the Student *t* test with a two-tail distribution. Comparisons with *P* values <0.05 were considered significant. Effect size (β) was calculated by subtracting the mean difference between two groups, and dividing the result by the pooled SD: $\beta = (M_2 - M_1)SD_{pooled}$, $SD_{pooled} = \sqrt{([SD_1^2 + SD_2^2]2)}$, where M is the mean.

Data and Resource Availability

All data generated or analyzed during this study are included in the published article (and its online Supplementary Material).

RESULTS

Adipocyte-Specific Deletion of KLF14 Modifies Adiposity and Insulin and Lipid Levels in Female Mice

Adipocyte-specific *Klf14*-KO (*Klf14*$^{fl/fl}$*Adipoq*-Cre^{+} or KO) mice were born at expected Mendelian ratios and were indistinguishable from wild-type (*Klf14*$^{fl/fl}$*Adipoq*-Cre^{-} or WT) littermates at birth. At 8 weeks of age, mice were placed on a 45% HFD (Research Diets D12079B). We measured body weights over a 12-week period (Fig. 1*A*). Female *Klf14*$^{fl/fl}$*Adipoq*-Cre^{+} mice showed similar body weight increases as WT littermates. However, male *Klf14*-deficient mice had lower body weight starting at 8 weeks on the HFD (with 8% difference after 12 weeks on HFD, $P = 0.018$) (Fig. 1*B*, left). In humans, lower KLF14 expression is associated with higher visceral fat mass (1). To determine whether loss of KLF14 in adipocytes affected adiposity on the HFD, we measured body composition using EchoMRI (Fig. 1*A*). We found higher fat mass relative to lean mass in female *Klf14*$^{fl/fl}$*Adipoq*-Cre^{+} mice, while in male mice, we observed the opposite (Fig. 1*B*, middle and right). When determining individual organ weights normalized to tibia length, we found no differences between WT and *Klf14*-deficient mice for most organs, including brain, heart, kidney, muscle, spleen, and pancreas (Supplementary Fig. 2). However, we observed that parametrial-periovarian fat depots in female *Klf14*-deficient mice were 70% larger ($\beta_{perigonadal} = 1.105$, $P_{perigonadal} = 0.02$), whereas subcutaneous and epididymal fat depots of male *Klf14*-deficient mice were 33% and 27% smaller compared with WT littermates ($\beta_{subq} = -1.073$, $P_{subq} = 0.01$; $\beta_{epididymal} = -1.006$, $P_{epididymal} = 0.01$) (Fig. 1*C*). Notably, adipocyte *Klf14* deficiency resulted in decreased liver weight in males and a trend toward a decrease in females ($\beta_{male} = -0.626$, $P_{male} = 0.05$; $\beta_{female} = -0.639$, $P_{female} = 0.18$) (Fig. 1*C*).

In humans, lower KLF14 expression in adipose tissue is associated with higher serum insulin and lower HDL levels, with a stronger effect in females (1). Consistent with this, we observed 78% higher insulin and 25% lower HDL levels in *Klf14*-deficient female but not in male mice after a 6-h fast ($\beta_{female,\ insulin} = 0.947$, $P_{female,\ insulin} = 0.036$; $\beta_{female,\ HDL} = 1.352$, $P_{female,\ HDL} = 0.004$) (Fig. 1*D* and *E*). Total cholesterol and NEFA were lower by 19% and 26%, while TG levels were 10% higher in female mice with adipocyte *Klf14* deficiency ($\beta_{female,\ cholesterol} = 1.176$, $P_{female,\ cholesterol} = 0.011$; $\beta_{female,\ NEFA} = 1.173$, $P_{female,\ NEFA} = 0.031$, $\beta_{female,\ TG} = 1.250$, $P_{female,\ TG} = 0.044$) (Fig. 1*F–H*). Mutant male mice also had lower NEFA levels ($\beta_{male,\ NEFA} = 1.022$, $P_{male,\ NEFA} = 0.01$) (Fig. 1*G*) but normal serum cholesterol and TG levels (Fig. 1*F* and *H*).

Adipocyte-Specific Deletion of KLF14 Affects Adipocyte Size

The parametrial-periovarian fat depot in female mice and the epididymal fat depot in male mice are considered visceral fat. Larger visceral fat depots with bigger adipocytes are a significant risk factor for T2D, cardiovascular disease, and hypertension (24,25). Adipocyte size is increased in obese conditions (26,27). To test whether adipocyte size was altered as a result of *Klf14* deficiency, we performed histological analysis using hematoxylin and eosin staining of subcutaneous and perigonadal fat depots (Fig. 2*A*). We observed that adipocyte size in female mice with adipocyte deletion of *Klf14* was 25% smaller in the subcutaneous depot ($\beta_{subq} = -0.422$, $P_{subq} = 4.02 \times 10^{-85}$) and 70% larger in the parametrial-periovarian depot relative to WT mice ($\beta_{periovarian} = 0.706$, $P_{periovarian} = 2.25 \times 10^{-175}$) (Fig. 2*B*). In contrast, adipocyte size in male mice with adipocyte deletion of *Klf14* was 6% larger in the subcutaneous depot ($\beta_{subq} = 0.09$, $P_{subq} = 1.66 \times 10^{-3}$) and 14% smaller in the epididymal depot relative to WT mice ($\beta_{epididymal} = -0.233$, $P_{epididymal} = 2.66 \times 10^{-15}$) (Fig. 2*B*). These findings suggest that KLF14 regulates adipocyte size and adipose tissue mass in a depot-specific and sex-specific manner.

Deletion of KLF14 in Adipocytes Causes Increased Insulin Resistance in Female Mice

Adipose tissues regulate systemic glucose metabolism and insulin sensitivity (28,29). Genetic studies showed that T2D risk alleles associated with lower KLF14 expression in adipose tissue led to higher fasting insulin in humans, indicating decreased insulin sensitivity (1,5). As described above, we also observed increased insulin levels in female *Klf14*-deficient mice (Fig. 1*D*). To further explore whether the differences in adipose tissue mass as a result of *Klf14* deletion in adipocytes affected systemic glucose homeostasis and insulin sensitivity, we performed glucose and insulin tolerance tests with intraperitoneal injections of glucose or insulin after 7 and 9 weeks of the HFD, respectively. Mice with adipocyte-specific *Klf14* deletion had a similar response to an intraperitoneal glucose bolus as WT littermates (Fig. 3*A*). However, in the insulin tolerance test, female mice with adipocyte-specific *Klf14* deletion displayed increased glucose levels compared with WT littermates, with 19% higher calculated area under the curve (AUC) ($\beta_{AUC} = 1.233$, $P_{AUC} = 0.005$) (Fig. 3*B*) indicating increased insulin resistance. Insulin sensitivity for

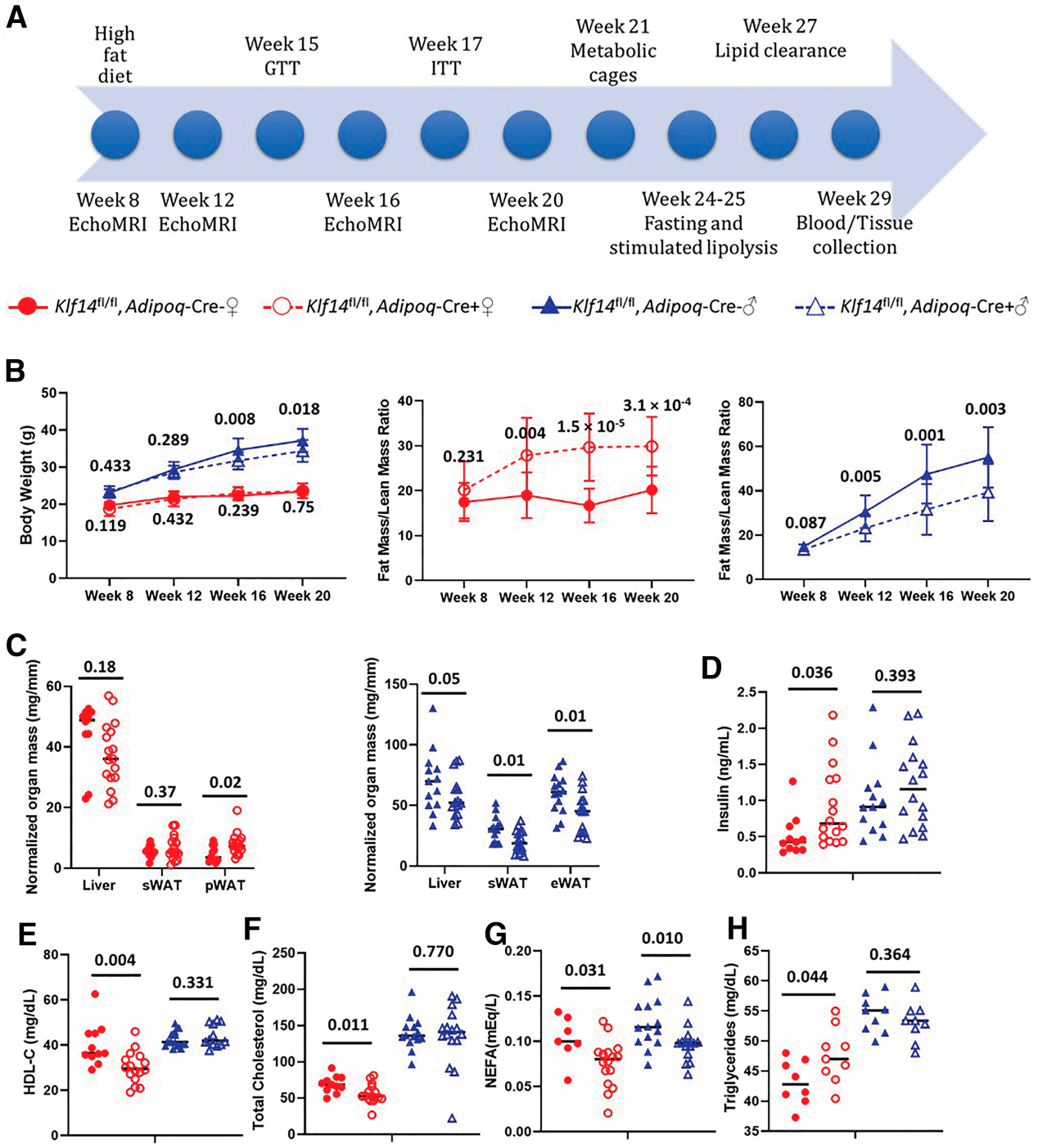

Figure 1—Adipocyte-specific deletion of KLF14 increases fat mass and affects circulating insulin and lipid levels in female mice. *A*: Experimental design for the metabolic characterization of mice. GTT, glucose tolerance test; ITT, insulin tolerance test. *B*: Body weight (left), fat mass–to–lean mass ratios in female (♀, red) (middle, $n_{Adipoq\text{-}Cre-} = 11$, $n_{Adipoq\text{-}Cre+} = 17$) and male (♂, blue) (right, $n_{Adipoq\text{-}Cre-} = 14$, $n_{Adipoq\text{-}Cre+} = 14$) mice at 8, 12, 16, and 20 weeks of age. *C*: Normalized organ weights in female (left, $n_{Adipoq\text{-}Cre-} = 11$, $n_{Adipoq\text{-}Cre+} = 17$) and male mice (right, $n_{Adipoq\text{-}Cre-} = 14$, $n_{Adipoq\text{-}Cre+} = 14$). Plasma/serum levels of insulin (*D*), HDL-C (*E*), total cholesterol (*F*), NEFA (*G*), and TG (*H*) in female ($n_{Adipoq\text{-}Cre-} = 8$–$11$, $n_{Adipoq\text{-}Cre+} = 9$–$17$) and male ($n_{Adipoq\text{-}Cre-} = 9$–$14$, $n_{Adipoq\text{-}Cre+} = 9$–$14$) mice at 29 weeks of age after 6 h of fasting. Data shown in *B* are mean ± SEM and in *C*–*H* are mean and data for individual mice. *P* values were calculated using two-tailed unpaired Student *t* tests at each time point for *B* and all data in *C*–*H*.

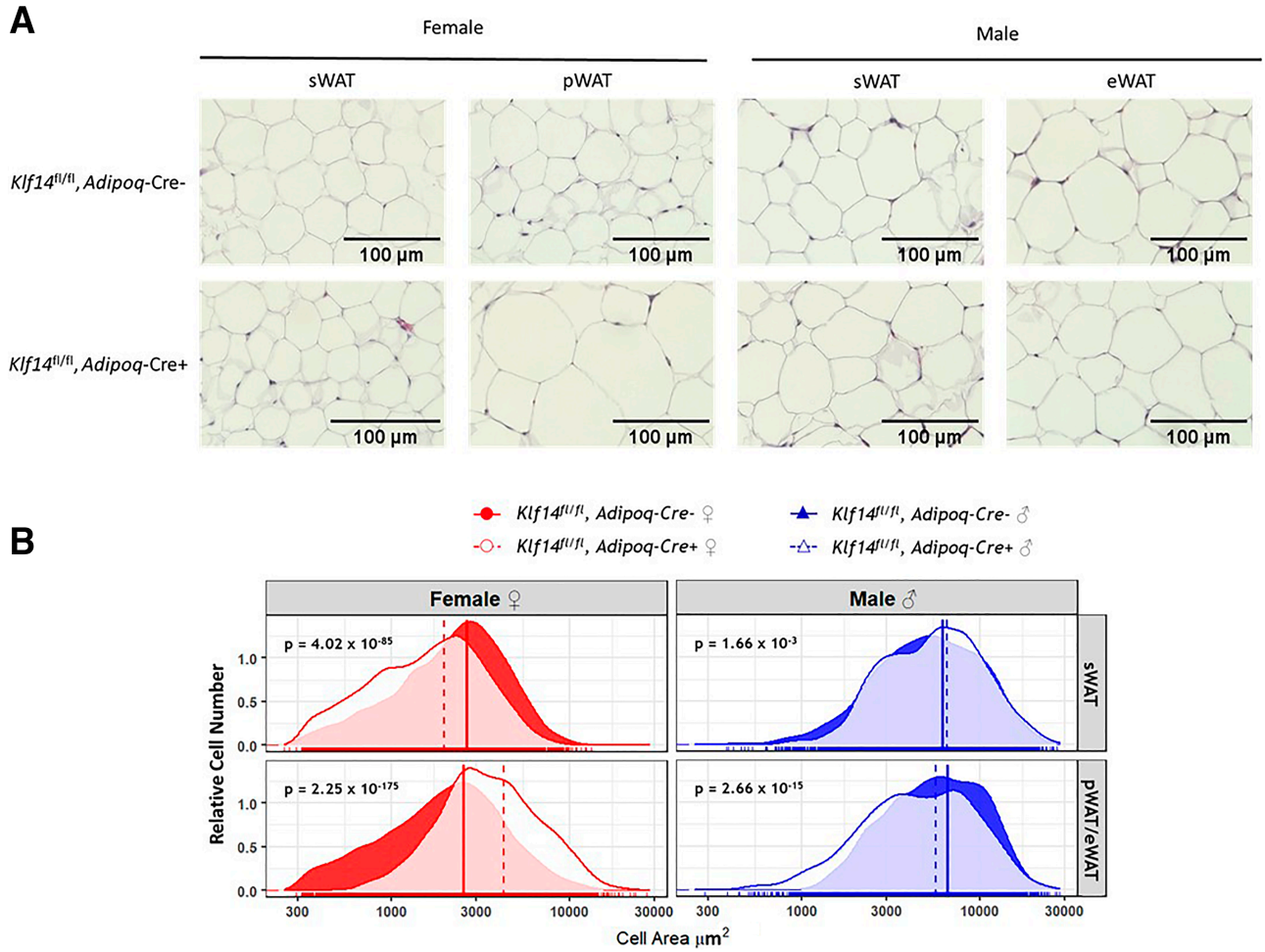

Figure 2—Adipocyte-specific deletion of KLF14 affects adipocyte size in female mice. *A*: Representative sWAT and visceral (pWAT/eWAT) adipose tissue sections stained with hematoxylin and eosin. *B*: Adipocyte size distribution in sWAT and visceral fat depots (pWAT/eWAT) of female (♀ red) and male (♂ blue) mice. Tissue sections (5 μm thick) from four mice for each genotype and sex were used for the analysis. The number of cells analyzed was as follows: $n_{\text{Female\_Adipoq-Cre−\_sWAT}} = 3{,}988$; $n_{\text{Female\_Adipoq-Cre+\_sWAT}} = 5{,}193$; $n_{\text{Female\_Adipoq-Cre−\_pWAT}} = 4{,}132$; $n_{\text{Female\_Adipoq-Cre+\_pWAT}} = 3{,}218$; $n_{\text{Male\_Adipoq-Cre−\_sWAT}} = 2{,}699$; $n_{\text{Male\_Adipoq-Cre+\_sWAT}} = 2{,}191$; $n_{\text{Male\_Adipoq-Cre−\_eWAT}} = 2{,}196$; and $n_{\text{Male\_Adipoq-Cre+\_eWAT}} = 2{,}435$ cells. *P* values were calculated using two-tailed unpaired Student *t* tests.

male mutant mice was similar to WT ($\beta_{AUC} = 0.027$, $P_{AUC} = 0.943$) (Fig. 3*B*).

Deletion of KLF14 in Adipocytes Modifies Energy Metabolism in Female Mice

Increased fat mass in female mice with *Kl14* deficiency suggested a defect in energy balance. To investigate the role of KLF14 in energy homeostasis, we performed indirect calorimetry studies using metabolic cages. Food consumption was comparable between *Klf14*-deficient and WT mice (Supplementary Fig. 4), and mice of both genotypes maintained body weights within 5–10% of their initial weight during the 3-day period in the metabolic cages. Despite these similarities, female *Klf14*$^{fl/fl}$*Adipoq*-Cre^{+} mice showed a 38% decrease in locomotor activity ($\beta_{\text{locomotor activity}} = 2.212$, $P_{\text{locomotor activity}} = 5.2 \times 10^{-4}$) compared with WT mice during the dark cycle (Fig. 4*A*). V_{O_2} was lower in both the light and dark cycles by 26% and 19%, respectively ($\beta_{O2,\ dark} = 2.320$, $P_{O2,\ dark} = 0.003$; $\beta_{O2,\ light} = 1.569$, $P_{O2,\ light} = 0.0095$), whereas CO_2 release was 14% lower in the light cycle and trended toward a decrease in the dark cycle ($\beta_{CO2,\ dark} = 0.900$, $P_{CO2,\ dark} = 0.093$; $\beta_{CO2,\ light} = 1.262$, $P_{CO2,\ light} = 0.026$) (Fig. 4*B* and *C*). The calculated RER (RER = V_{CO_2}/V_{O_2}), an indicator for the metabolic energy source (carbohydrate or fat), was higher (close to 1) for female *Klf14*$^{fl/fl}$*Adipoq*-Cre^{+} mice than for WT littermates ($\beta_{RER,\ dark} = 4.258$, $P_{RER,\ dark} = 1.0 \times 10^{-6}$) in the dark cycle (Fig. 4*D*), suggesting predominant use of carbohydrates as an energy source, despite being fed the HFD. The indirect calorimetry measurements allowed us to estimate consumed substrates using the gas exchange ratios as a surrogate for substrate use (16). Female *Klf14*$^{fl/fl}$*Adipoq*-Cre^{+} mice had 82% higher carbohydrate use ($\beta_{\text{carbohydrate, dark}} = 2.015$, $P_{\text{carbohydrate, dark}} = 0.01$) and 79% decreased fat use ($\beta_{\text{fat, dark}} = -5.400$, $P_{\text{fat, dark}} = 1.1 \times 10^{-6}$) in the dark cycle compared with WT mice. We

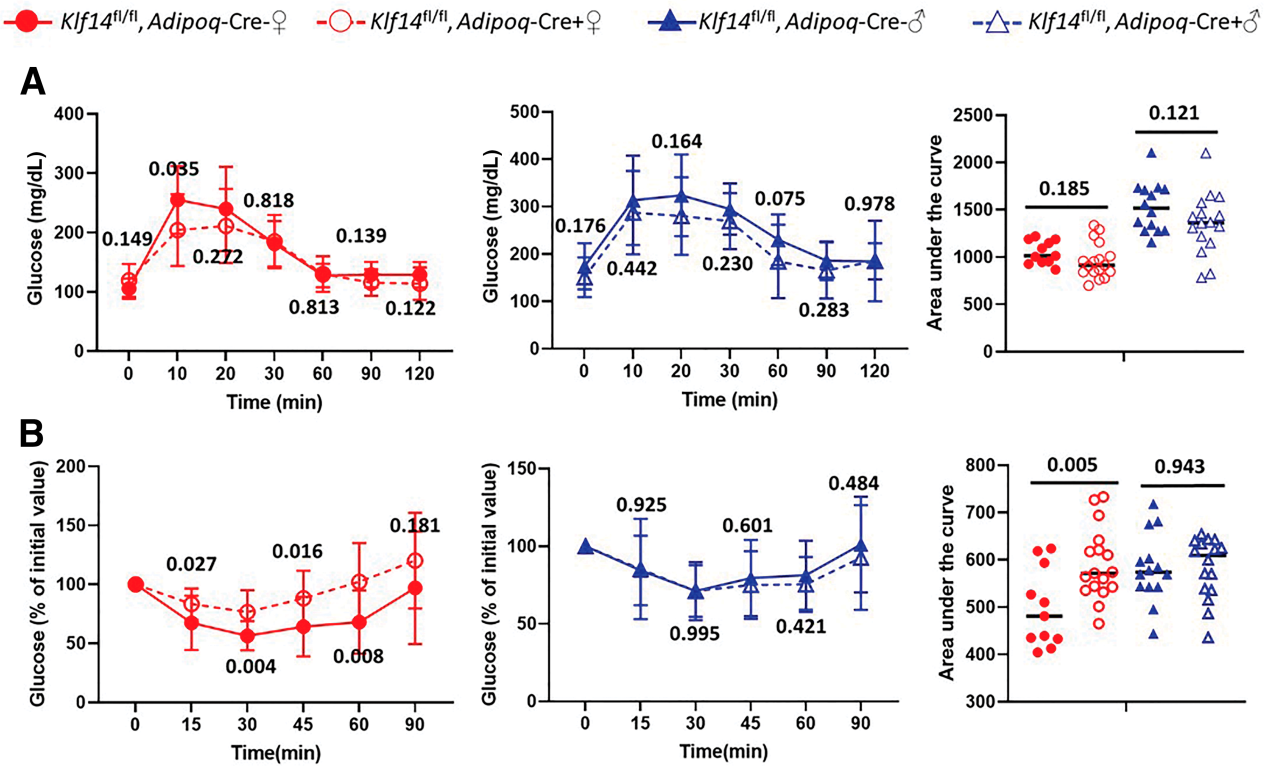

Figure 3—Adipocyte-specific deletion of KLF14 leads to increased insulin resistance in female mice. Blood glucose concentrations during intraperitoneal glucose tolerance tests after 7 weeks of HFD (*A*) and insulin tolerance tests after 9 weeks of HFD (*B*) in female (♀, red; left) and male mice (♂, blue; middle). Graphs for the AUC blood glucose concentrations are shown (right). $n_{\text{Female\_Adipoq-Cre}-} = 11$, $n_{\text{Female\_Adipoq-Cre}+} = 17$, $n_{\text{Male\_Adipoq-Cre}-} = 14$, $n_{\text{Male\_Adipoq-Cre}+} = 14$. Data are mean ± SEM. *P* values were calculated using two-tailed unpaired Student *t* tests at each time point.

did not observe differences for any of the measured parameters for male mice in dark or light cycles (Fig. 4).

Deletion of KLF14 in Adipocytes Causes Defects in Lipid Metabolism in Female Mice

We reasoned that defects in lipid breakdown (lipolysis) or lipid uptake and synthesis (lipogenesis) in adipocytes could explain the shift in energy source for female mice. Compatible with these possibilities, circulating NEFA and TG levels were decreased and increased under fasting conditions, respectively, in female mutant mice (Figs. 1*G* and *H*). To follow-up on these changes, we first measured lipolytic products, NEFAs, and glycerol after 16 h of fasting. NEFA levels increased as a result of fasting, as expected (Fig. 5*A*). However, female *Klf14*$^{\text{fl/fl}}$*Adipoq*-Cre^{+} mice had 17% and 38% lower NEFA levels compared with WT littermates in fed and fasted states ($\beta_{\text{fed}} = -1.416$, $P_{\text{fed}} = 0.013$; $\beta_{\text{fasted}} = -3.231$, $P_{\text{fasted}} = 1 \times 10^{-4}$) (Fig. 5*A*), with NEFA levels in *Klf14*-deficient female mice increasing to a lesser extent compared with WT littermates in response to fasting ($\beta = -1.292$, $P = 0.021$) (Fig. 5*B*). Glycerol in female mice was only decreased in the fed state ($\beta_{\text{fed}} = 2.157$, $P_{\text{fed}} = 7 \times 10^{-4}$) (Fig. 5*C* and *D*). No differences in NEFA and glycerol were observed in male mice, except that NEFAs under fed conditions were slightly increased ($P = 0.036$) (Fig. 5).

Adipocyte lipolysis is regulated by hormonal and neuronal stimulation (30), with β-adrenergic receptor signaling potently increasing lipolysis (31). To further corroborate that female mice with *Klf14*-deficient adipocytes indeed had a defect in lipolysis, we quantified serum levels of NEFA and glycerol in response to isoproterenol that stimulates β-1 and β-2 adrenergic receptors (32). Female *Klf14*$^{\text{fl/fl}}$*Adipoq*-Cre^{+} mice had 21% and 22% lower NEFA levels compared with WT littermates under the fed condition in nonstimulated and stimulated states, respectively ($\beta_{\text{nonstimulation}} = -2.692$, $P_{\text{nonstimulation}} = 9 \times 10^{-5}$; $\beta_{\text{stimulated}} = -2.699$, $P_{\text{stimulated}} = 8 \times 10^{-5}$) (Fig. 5*E*), with NEFA levels in *Klf14*-deficient female mice increasing to a lesser extent than in WT littermates in response to stimulation ($\beta = -1.022$, $P = 0.06$) (Fig. 5*F*). No differences were observed in male mice (Fig. 5*E* and *F*). Similar to fasting experiments, we observed a difference in the serum glycerol level in female mice before stimulation ($\beta_{\text{female}} = -0.307$, $P_{\text{female}} = 0.021$) but not after ($\beta_{\text{female}} = -0.301$, $P_{\text{female}} = 0.559$) (Fig. 5*G*). Changes in serum glycerol levels upon stimulation did not differ between genotypes in both female and male mice ($\beta_{\text{female}} = 0.815$,

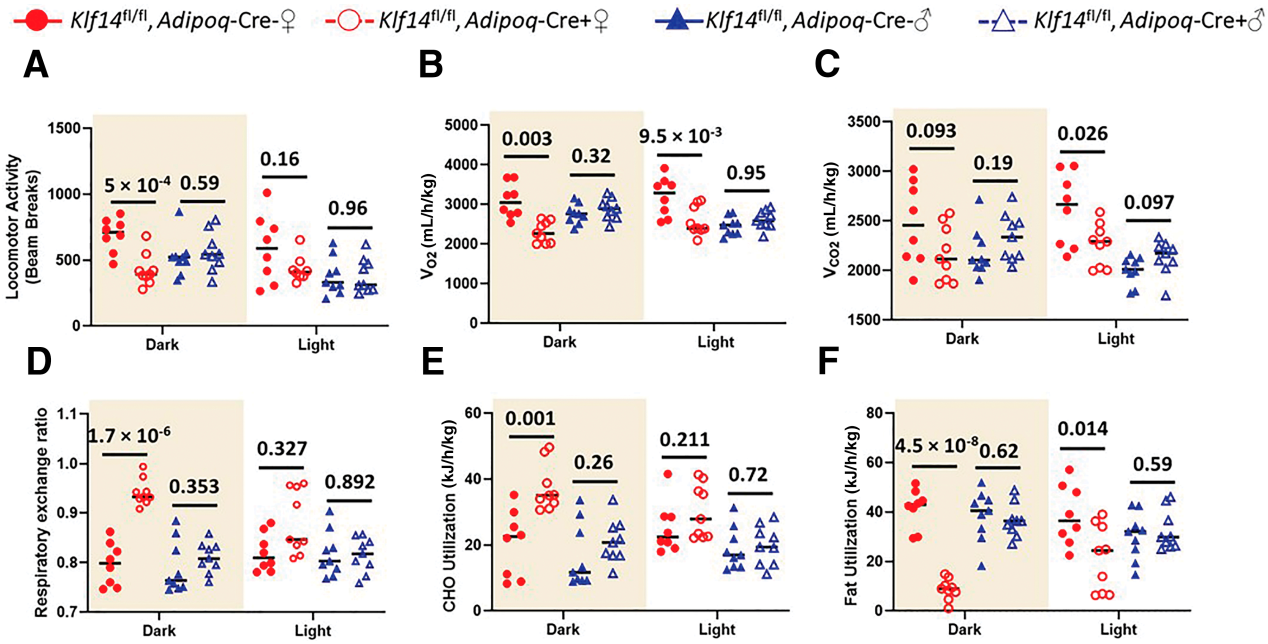

Figure 4—Adipocyte-specific deletion of KLF14 modifies energy metabolism in female mice. Indirect calorimetry studies measuring total activity (*A*), V_{O_2} (*B*), V_{CO_2} (*C*), RER (*D*), carbohydrate (CHO) use (*E*), and fat use (*F*) in female (♀, red) and male (♂, blue) mice during dark (shaded area) and light cycles ($n_{\text{Female\_Adipoq-Cre}-} = 8$, $n_{\text{Female\_Adipoq-Cre}+} = 9$, $n_{\text{Male\_Adipoq-Cre}-} = 9$, $n_{\text{Male\_Adipoq-Cre}+} = 9$). Mean and individual mouse data are shown. *P* values were calculated using two-tailed unpaired Student *t* tests.

$P_{female} = 0.166$; $\beta_{male} = -0.031$, $P_{male} = 0.951$) (Fig. 5*H*). The difference in NEFA and glycerol responses to induced lipolysis is most likely due to different metabolic fates of NEFA and glycerol after release into the circulation.

Given that the adipocyte size changed in opposite directions in subcutaneous and visceral depots, we tested whether differences in cell size are caused by differences in lipolysis. We assessed lipolysis with and without isoproterenol stimulation ex vivo using adipocytes isolated from subcutaneous and visceral depots. We observed that female *Klf14*-deficient compared with WT adipocytes showed decreased lipolysis irrespective of whether they were derived from subcutaneous or visceral depots (Fig. 5*I* and *J*). However, nonstimulated lipolysis was more drastically reduced in visceral than in subcutaneous *Klf14*-deficient adipocytes. There was no significant difference between *Klf14*-deficient and WT adipocytes from male mice (Fig. 5*I* and *J*). This suggests that the difference between subcutaneous and visceral adipocyte size is caused by other processes, such as differential changes in lipid uptake and synthesis (see below and Fig. 6*F* and *G*).

TG hydrolysis to NEFA and glycerol is achieved in a three-step enzymatic pathway (Fig. 5*I*). We measured the expression of adipocyte TG lipase (ATGL), the first enzyme in the TG breakdown pathway, and found that mRNA levels of *Pnpla2* in adipocytes isolated from subcutaneous and parametrial-periovarian/epididymal fat were decreased by 24% and 29%, respectively, as a result of *Klf14* deficiency in female mice ($\beta_{sWAT} = -9.320$, $P_{sWAT} = 5 \times 10^{-3}$; $\beta_{pWAT} = -13.139$, $P_{pWAT} = 1 \times 10^{-4}$) (Fig. 5*J*), but were normal in male mice. We also measured HSL, the second enzyme in the TG breakdown pathway, but did not observe differences in *Lipe* mRNA expression in adipocytes of male or female mice (Fig. 5*K*). HSL activity is predominantly regulated by phosphorylation (33). We thus measured pHSL levels in adipocytes isolated from subcutaneous and visceral depots following isoproterenol stimulation. We observed that pHSL was reduced in *Klf14*-deficient adipocytes isolated from visceral and subcutaneous depots of both female and male mice (Fig. 5*N* and *O*). Lower *Pnpla2* expression together with decreased pHSL is consistent with the above-described decreased lipolysis and increased fat mass and adipocyte size of visceral adipocytes in female mutant mice. Normal *Pnpla2* expression in male *Klf14*-deficient adipocytes is associated with normal levels of lipolysis despite decreased pHSL. Visceral adipocytes are normally more lipolytically active compared with subcutaneous adipocytes (34).

Our metabolic cage data indicated that female *Klf14*$^{fl/fl}$ *Adipoq*-Cre^{+} mice were not able to efficiently use dietary fatty acids, leading us to speculate that there was also a defect in lipid uptake. Therefore, we challenged mice with a bolus of olive oil by oral gavage and measured TG and NEFA levels to quantify lipid clearance from the bloodstream. We observed that blood TG and NEFA clearance were both decreased in female mutant mice compared with WT mice ($\beta_{4\ h\text{-}TG} = 4.610$, $P_{4\ h\text{-}TG} = 7.2 \times 10^{-9}$;

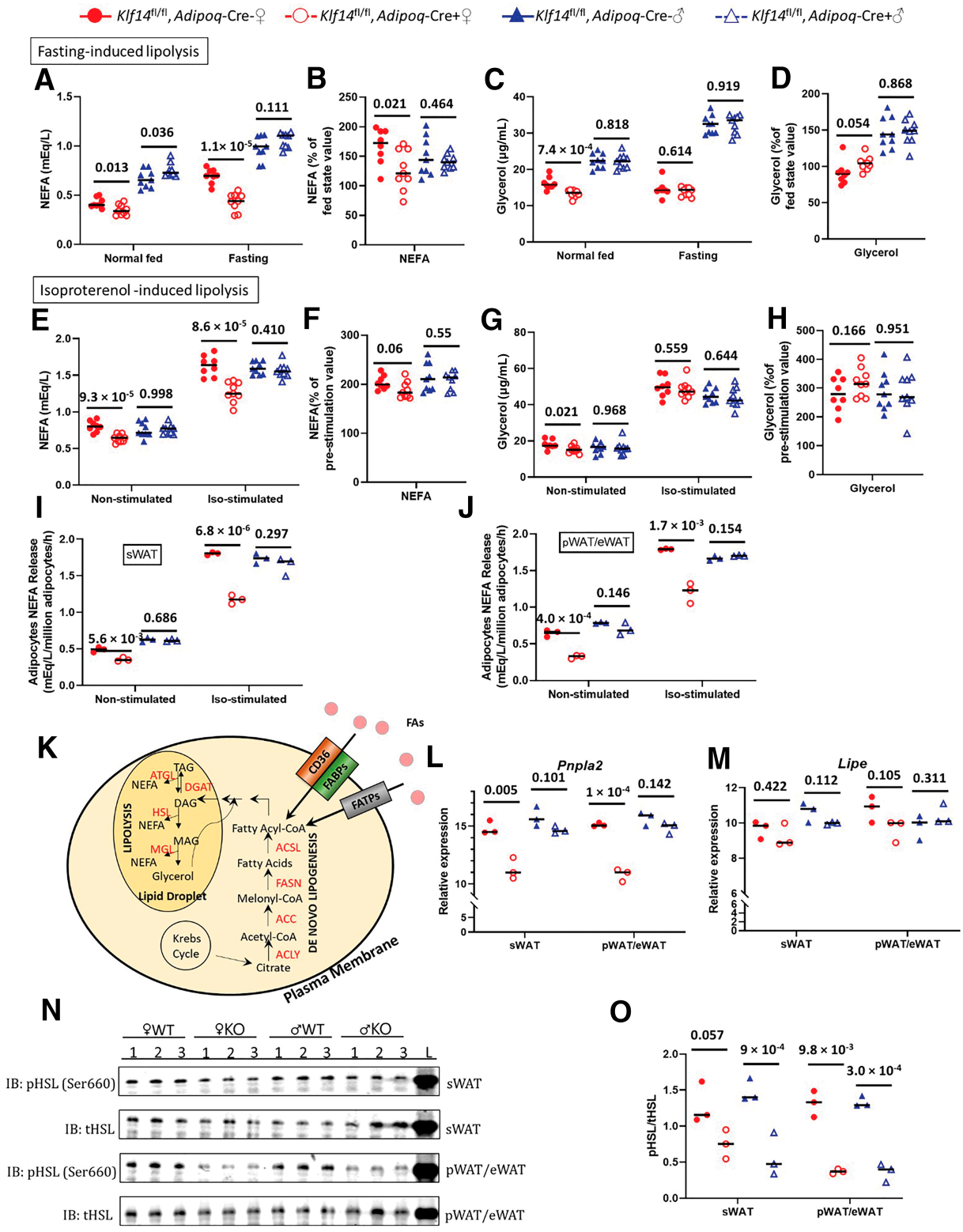

Figure 5—Adipocyte-specific deletion of KLF14 causes defects in lipolysis in female mice. Mice after a 16-week HFD were fasted for 16 h. Fasting NEFA (*A* and *B*) and glycerol (*C* and *D*) were measured and compared with that of mice before fasting. ♀, female; ♂, male. Mice after a 17-week HFD were treated with 10 mg/kg isoproterenol. Plasma NEFA (*E* and *F*) and glycerol (*G* and *H*) were measured and compared with that of mice before stimulation ($n_{\text{Female\_Adipoq-Cre}-} = 8$, $n_{\text{Female\_Adipoq-Cre}+} = 9$, $n_{\text{Male\_Adipoq-Cre}-} = 9$, $n_{\text{Male\_Adipoq-Cre}+} = 9$). Changes in plasma levels of NEFA and glycerol were calculated relative to baseline values (fed-state for *B* and *D* or before stimulation for *F* and *H*). Mean and individual mouse data are shown. *P* values were calculated using two-tailed unpaired Student *t* tests. Data from female mice (♀) are shown in red and male mice (♂) are shown in blue. Ex vivo lipolysis was assayed with and without isoproterenol stimulation using adipocytes isolated from subcutaneous (*I*) and pWAT/eWAT (*J*) depots. Adipocytes NEFA release was compared between nonstimulated and stimulated conditions in female and male WT and *Klf14*-deficient mice ($n_{\text{Female\_Adipoq-Cre}-} = 3$, $n_{\text{Female\_Adipoq-Cre}+} = 3$, $n_{\text{Male\_Adipoq-Cre}-} = 3$, $n_{\text{Male\_Adipoq-Cre}+} = 3$). *K*:

$\beta_{4\ \text{h-NEFA}} = 3.528$, $P_{4\ \text{h-NEFA}} = 8 \times 10^{-6}$) (Fig. 6*A* and *B*), consistent with decreased use of lipids as an energy source in female *Klf14*-deficient mice. No differences were observed in male mice (Fig. 6*C* and *D*). These results are consistent with our metabolic cage data that female mice use less fat as their energy source.

Uptake of fatty acids into cells is achieved predominantly via a saturable protein-facilitated process (35) (Fig. 5*I*). Several proteins facilitate the uptake of fatty acids, among which the best characterized are CD36, FABPs, and FATPs (36–38). Fatty acids are also synthesized in cells through de novo lipogenesis that is catalyzed by ATP-citrate lyase (encoded by *Acly*) (39), acetyl-CoA carboxylase (encoded by *Acaca* and *Acacb*) (40), and fatty acid synthase (encoded by *Fasn*) (41). Fatty acids are converted into fatty acyl-CoAs by acyl-CoA synthetase (encoded by *Acsl*) and then esterified with glycerol to form TGs, with the last step catalyzed by diglyceride acyltransferase (encoded by *Dgat*) (42). We assayed several key enzymes in adipocyte fatty acid uptake and lipogenesis and observed sex- and depot-specific differences in *Fabp4*, *Fatp4*, and *Dgat1* mRNA expression in isolated mature adipocytes. *Fabp4* was 36% lower in the parametrial-periovarian depot of female *Klf14*-deficient mice ($\beta_{\text{female pWAT}} = -10.750$, $P_{\text{female pWAT}} = 3 \times 10^{-4}$) (Fig. 6*E*), while *Fatp4* (Fig. 6*F*) and *Dgat1* (Fig. 6*G*) were 20% and 54% higher in the parametrial-periovarian depot of the same mice compared with WT controls ($\beta f_{\text{emale pWAT}} = 14.336$, $P_{\text{female pWAT}} = 8 \times 10^{-5}$). We also observed differences in other pathway genes that were either sex- or depot-specific. mRNA levels for *Fatp1* were decreased in both female sWAT and pWAT/visceral WAT, *Dgat2* was decreased in male sWAT and eWAT/visceral WAT. We also observed that Fabp5 was decreased in both female and male sWAT and visceral WAT (Supplementary Fig. 4). *Acaca*, *Acacb*$^{-}$, and *Fasn* showed no differences. (Supplementary Fig. 4).

Adipocyte KLF14 Overexpression Reduces Body Fat in Female Mice

Our results showed that KLF14 deficiency resulted in an adverse metabolic phenotype in female mice. We therefore hypothesized that overexpression of *Klf14* may be metabolically beneficial. To address this, we generated a transgenic mouse with *Klf14* overexpression under the regulation of the *Adipoq* promoter (*Adipoq-Klf14*-OE) (see *Research Design and Methods* section for a detailed description). This resulted in 1.7-fold induction of KLF14 in adipocytes (Supplementary Fig. 1*C*). We fed these mice the HFD for 18 weeks and performed body composition analysis using EchoMRI. Male and female mice from both genotypes gained similar amounts of body weight, and no differences in body weight between the *Klf*14-OE mice (*Adipoq-Klf14*-OE) and WT littermates were observed at the end of the 18-week diet challenge (Fig. 7*A*). However, starting at 12 weeks of the HFD, female *Adipoq-Klf14*-OE mice showed a trend toward decreased fat mass–to–lean mass ratios compared with WT littermates ($P = 0.074$) (Fig. 7*B*). At the end of the study, after 18 weeks of the HFD, female mice with *Klf14* overexpression in adipocytes had 38% lower body fat compared with WT littermates ($\beta_{\text{female}} = -1.446$, $P_{\text{female}} = 0.002$) (Fig. 7*B*). No differences were observed in male mice with *Klf14* overexpression ($P = 0.99$) (Fig. 7*C*).

Potential Sex-Dependent Action of KLF14

Sex hormones play a significant role in sex-specific body fat distribution, as evidenced by the fact that android and gynoid fat distribution patterns in males and females appear as early as puberty (43). Therefore, we measured the circulating levels of testosterone, progesterone, and estradiol after 29 weeks of HFD feeding. There was no significant difference between female and male mice with *Klf14*-deficient adipocytes and WT mice (Supplementary Fig. 5*A*), suggesting that the sex differences we observed in mice are likely hormone independent. It is, however possible that differential expression of sex hormone receptors or sex-specific interactions of KLF14 with sex hormone receptors could play a role in transcriptional target expression since other KLF family transcription factors have been shown to co-bind DNA with the estrogen receptor (44). Therefore, we tested the hypothesis that KLF14 interacts with estrogen receptor-α (ESR1). We overexpressed FLAG-tagged KLF14 (*KLF14-FLAG*) and HA-tagged ESR1(*ESR1-HA*) in HEK293 cells and performed immunoprecipitations with anti-FLAG antibody. Untransfected cells or cells that were only transfected with one of the two vectors served as negative controls.

Schematic representation of genes playing a role in TG breakdown (lipolysis) and formation (lipogenesis), and fatty acid uptake. Lipolysis is catalyzed by three lipases: ATGL, HSL, and monoacylglycerol lipase (MGL), whose actions result in the release of NEFA and glycerol. TG synthesis through de novo lipogenesis uses citrate to make acetyl-CoA by ATP-citrate lyase (ACL), acetyl-CoA is converted to malonyl-CoA by acetyl-CoA carboxylase (ACC), and fatty acid synthesis is achieved by conversion of malonyl-CoA into fatty acids by fatty acid synthase (FASN). Fatty acids are then made into fatty acyl-CoAs by acyl-CoA synthetase (ACSL) and converted to diacylglycerols (DAG) through several enzymatic reactions. Diacylglycerol acyltransferase (DGAT) then catalyzes the conversion of DAG into TAG (triacylglycerol or TG). Cellular uptake of fatty acids (FAs) is facilitated by CD36, FABPs, and FATPs. mRNA expression of *Pnpla2* (*L*) and *Lipe* (*M*) in mature adipocytes isolated from sWAT and pWAT/eWAT ($n = 3$ mice per genotype and sex). Relative gene expression, normalized to GAPDH levels, was calculated using the $2^{-\Delta\Delta CT}$ method. *P* values were calculated using two-tailed unpaired Student *t* tests. *N*: pHSL and total HSL (tHSL) were measured in adipocytes isolated from subcutaneous and parametrial-periovarian/epididymal depot depots following isoproterenol stimulation in female and male WT and *Klf14*-deficient mice using Western blot ($n_{\text{Female\_Adipoq-Cre}-} = 3$, $n_{\text{Female\_Adipoq-Cre}+} = 3$, $n_{\text{Male\_Adipoq-Cre}-} = 3$, $n_{\text{Male\_Adipoq-Cre}+} = 3$). IB, immunoblotting. *O*: pHSL-to-tHSL ratio was quantified and compared.

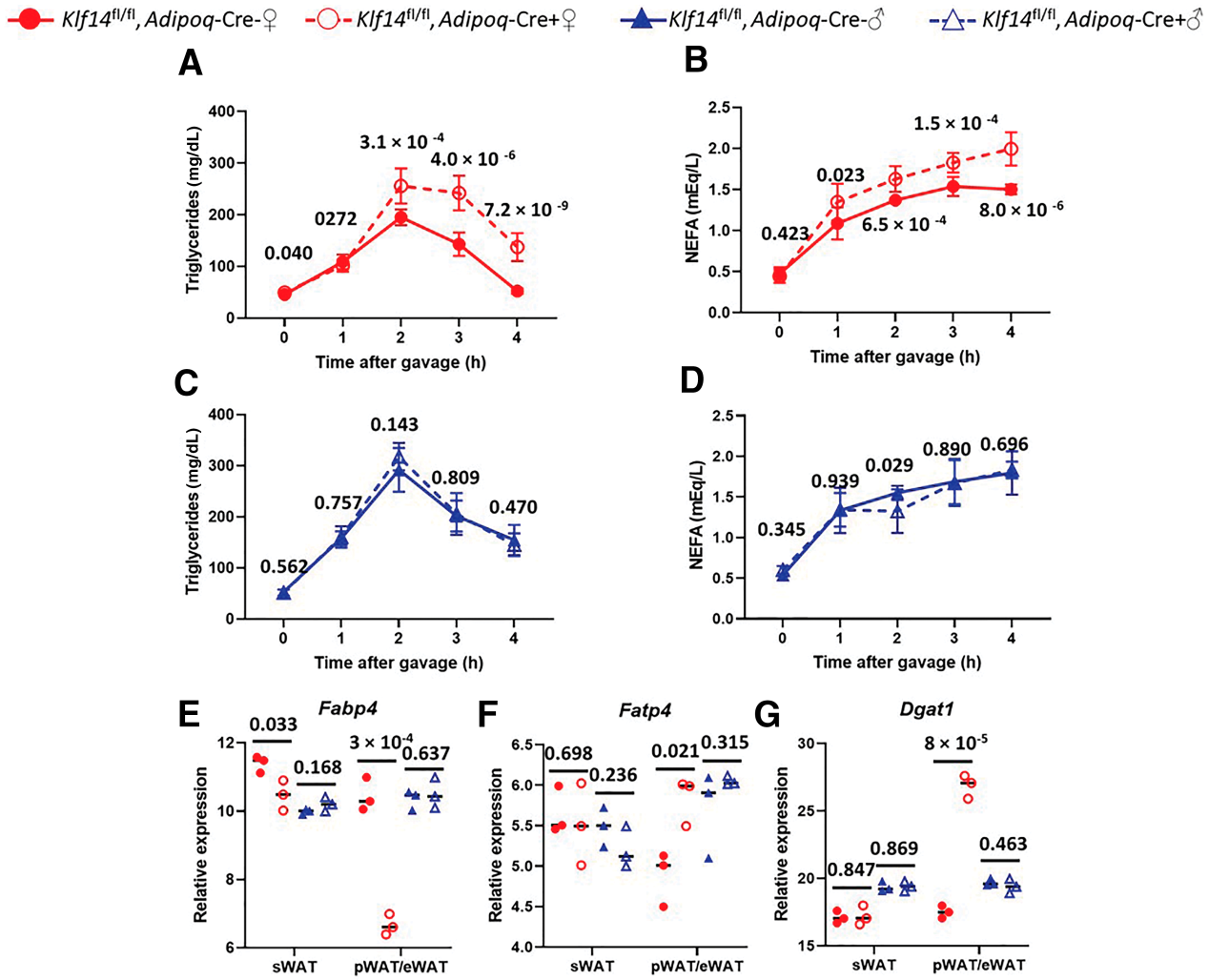

Figure 6—Adipocyte-specific deletion of KLF14 decreases lipid clearance in female mice. Mice fed the HFD for 19 weeks were gavaged with a bolus of olive oil. Plasma TG in female (♀) (*A*) and male (♂) mice (*C*) and NEFA in female (*B*) and male (*D*) mice were measured over 4 h ($n_{\text{Female\_Adipoq-Cre}-} = 8$, $n_{\text{Female\_Adipoq-Cre}+} = 9$, $n_{\text{Male\_Adipoq-Cre}-} = 9$, $n_{\text{Male\_Adipoq-Cre}+} = 9$. mRNA expression of fatty acid uptake gene *Fabp4* (*E*), *Fatp4* (*F*), and de novo lipogenesis gene *Dgat1* (*G*) was measured in mature adipocytes isolated from sWAT, pWAT, and eWAT ($n = 3$ mice per genotype and sex). Relative gene expression, normalized to GAPDH levels, was calculated using the $2^{-\Delta\Delta CT}$ method. Mean and SEM are shown in *A*, *B*, *C*, and *D*; mean and individual mouse data are shown in *E*, *F*, and *G*. *P* values were calculated using two-tailed unpaired Student *t* tests. Data from female mice are shown in red, and data for male mice are shown in blue.

We blotted the immunoprecipitated samples with anti-HA or anti-ESR1 antibodies, respectively. We detected the presence of ESR1 protein in the sample that overexpressed both KLF14 and ESR1 but not in negative control samples, suggesting that KLF14 can bind ESR1 (Supplementary Fig. 5*B* and *C*).

In summary (Fig. 8), *Klf14* deficiency in adipocytes caused major abnormalities in HFD-fed female but not male mice. Female mice with *Klf14*-deficient adipocytes had increased total body fat with larger visceral fat mass and bigger visceral adipocytes, but they had smaller subcutaneous adipocytes. Concomitant with the changes in body fat distribution and adipocyte size, the mice demonstrate metabolic abnormalities, including insulin resistance and altered serum lipid levels. Despite HFD feeding, *Klf14*-deficient female mice used carbohydrates as the predominant source of energy and simultaneously had lower energy expenditure and activity. Further evaluation of lipid metabolism uncovered defects in fasting- and β-adrenergic–induced lipolysis, and impaired TG and NEFA clearance after lipid gavage. These defects were coupled with decreased mRNA expression of *Pnpla2* (a key lipolytic enzyme) in both perigonadal/visceral and subcutaneous adipocytes and decreased pHSL. Furthermore, mRNA levels for proteins involved in cellular fatty acid uptake, including Fabp4, Fabp5, and Fatp1, were decreased in both sWAT and pWAT/visceral WAT, but mRNA levels of the fatty acid transport protein Fatp4 and Dgat1, an enzyme that catalyzes the conversion of DAG into TG, were increased only in perigonadal/visceral adipocytes. In

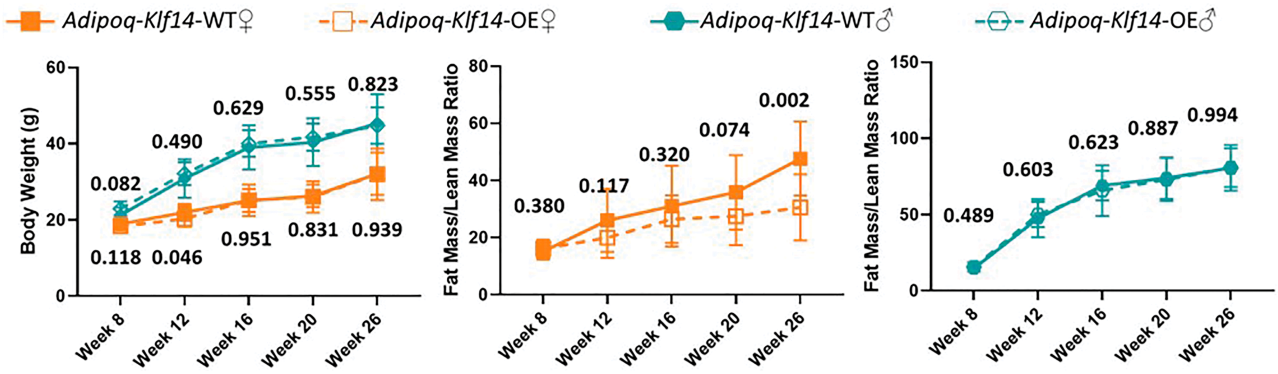

Figure 7—Adipocyte-specific OE of KLF14 decreases fat mass in female mice. Body weight (left), fat mass-to-lean mass ratio in female (♀, orange) (middle, $n_{WT} = 14$, $n_{Adipoq\text{-}OE} = 14$) and male (♂, blue) (right, $n_{WT} = 8$, $n_{Adipoq\text{-}OE} = 12$) mice at 8, 12, 16, 20, and 26 weeks of age. Data shown are mean ± SEM. *P* values were calculated using two-tailed unpaired Student *t* test at each time point.

contrast, male mice with *Klf14*-deficient adipocytes fed the HFD gained less body weight and had decreased total body fat with smaller epididymal/visceral and subcutaneous fat depots and adipocytes, but had, relative to WT, normal metabolic parameters and insulin sensitivity. The male mice did not show defects in stimulated lipolysis (despite decreased pHSL in pWAT) and lipid clearance, and mRNA levels of enzymes involved in cellular lipid metabolism were not different from WT littermates, except that Fatp1 was increased in sWAT, and Fabp5 and Dgat2 decreased in sWAT and eWAT/visceral WAT. In conclusion, our findings suggest that KLF14 regulates adipose tissue mass and adipocyte size in a depot-specific and sex-specific manner, most likely by differentially modifying adipocyte lipid metabolism.

DISCUSSION

Visceral adipose tissue expansion independent of overall adiposity is associated with an increased risk for developing T2D and cardiovascular disease (45). How deposition of excess calories into the different adipose depots is regulated is currently unknown. However, sex-dependent differences in adipose tissue distribution are well documented, with higher adiposity in women than men (46). Men usually display "android" or "apple shape" distribution, with more visceral fat in the abdominal region, while women have "gynoid" or "pear shape" distribution, with more subcutaneous fat and less visceral fat in the lower body (47). A shift in fat deposition from subcutaneous depots around the hip to visceral depots in the waist region in men confers increased risk for metabolic disorders (48). However, women can harbor increased upper-body fat without enhanced metabolic disease risk as excess fat is mainly stored in subcutaneous depots. Our results suggest that the transcription factor KLF14 plays a role in modifying adipocyte function and thereby adipose tissue distribution in a sex- and depot-specific manner. Deletion of the *Klf14* gene in mature adipocytes resulted in an increase of visceral fat in female mice but a decrease in male mice. The shift in lipid storage from subcutaneous to parametrial-periovarian (visceral) depots in female mice with adipocyte *Klf14* deletion was characterized by changes in adipocyte size, smaller adipocytes in subcutaneous and larger adipocytes in perigonadal/visceral adipose tissues, and major abnormalities in lipid metabolism.

Identifying the molecular mechanisms of how KLF14 affects adipocyte function in a sex-specific manner remains a challenge. Although we did not observe sex hormone differences at the end of our experiments, we cannot rule out the possibility that earlier differences during development exist. Further, we showed that when we overexpressed KLF14 and ESR1 in HEK293 cells, they can co-bind. However, this result needs to be verified for endogenous proteins in adipocytes, especially since HEK293 cells do not express ESR1.

The absence of *Klf14* in adipocytes causes significant abnormalities in lipid metabolism, both lipolysis and fatty acid uptake in female mice. Whether these are primary consequences of KLF14 deficiency or secondary metabolic abnormalities due to changes in adipose tissue mass and distribution and adipocyte size is not entirely clear. Future identification of the primary consequences of KLF14 deficiency on metabolism and primary KLF14 targets will require the careful analysis of metabolic phenotypes at various time points before and after the transition to a HFD. Abnormalities in circulating lipids in female mice with *Klf14* deficiency in adipocytes can partly be explained by the increased insulin resistance in female mice with *Klf14*-deficient adipocytes. This includes the lower circulating HDL-cholesterol (HDL-C) and increased plasma TG levels under fasting condition, and impaired TG and NEFA clearance after lipid gavage. TG clearance requires the action of lipoprotein lipase in adipose tissues, and insulin-stimulated lipoprotein lipase activity is impaired in insulin resistance. Insulin-stimulated NEFA uptake under fed conditions is also defective in insulin resistance. Furthermore, expression of fatty acid transporters is decreased in the presence of

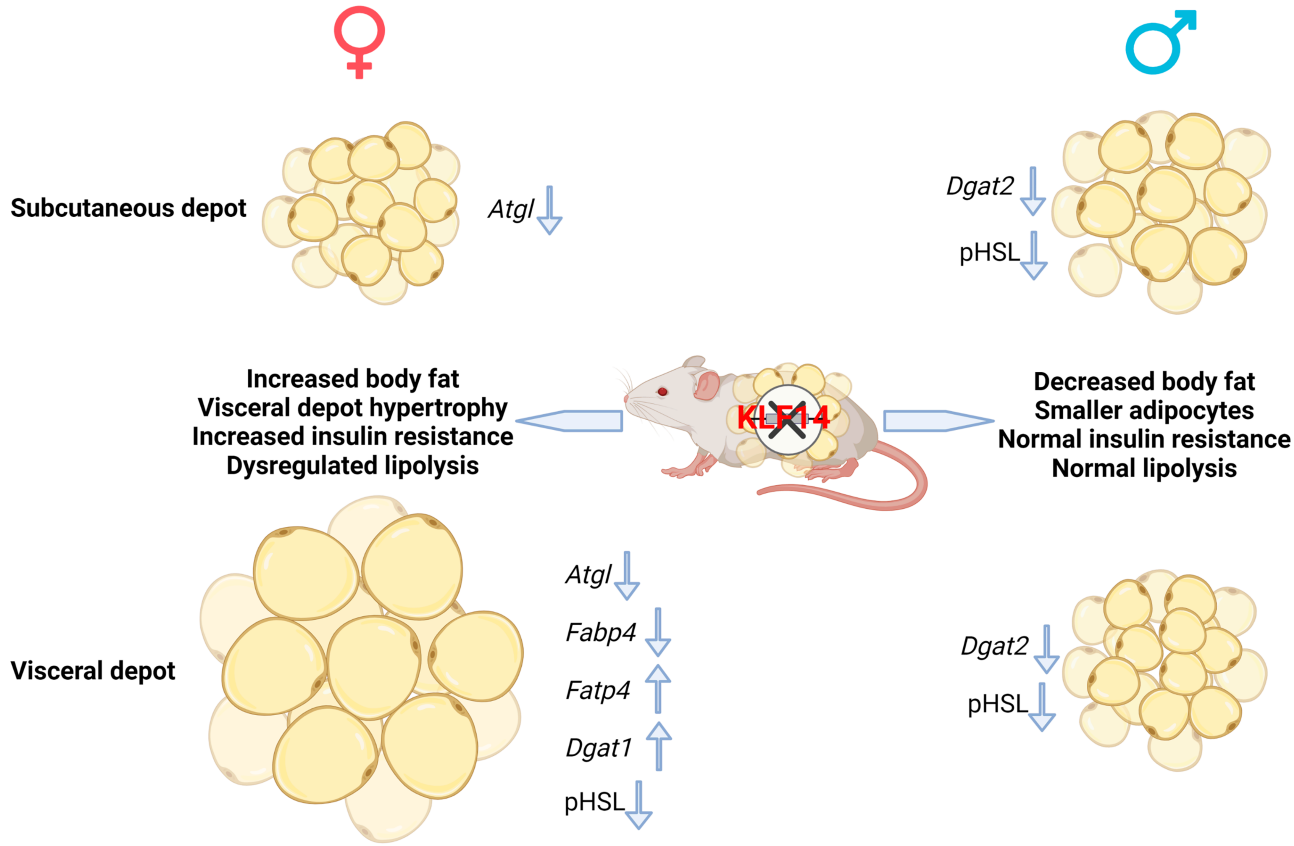

Figure 8—Summary of main findings. Deletion of KLF14 in mouse adipocytes resulted in sex-dimorphic and depot-specific differences. Female mice (♀) with adipocyte *Klf14* deficiency had higher total body fat, primarily due to increased visceral depot fat mass. Female mutant mice also displayed a shift in body fat storage from the subcutaneous depot to the visceral depot as evidenced by visceral adipocyte hypertrophy and decreased adipocyte size in subcutaneous depots. Meanwhile, male mice (♂) had lower body fat mass and smaller cell size in the visceral depots. Female *Klf14*-KO mice were insulin resistant, while insulin sensitivity in male mice with adipocyte *Klf14* deficiency was not different from WT littermates. Changes in adipose tissue mass and adipocyte size can, at least in part, be explained by dysregulation of lipid metabolism, including lipolysis, fatty acid uptake, and lipogenesis. Several genes involved in these pathways are dysregulated in a sex- and depot-specific manner as indicated. Figure created using BioRender (https://biorender.com/).

impaired insulin sensitivity (49). However, the lower-than-normal NEFA levels in female mice under fed and fasting conditions and in response to β-adrenergic stimulation cannot be attributed to impaired insulin sensitivity. On the contrary, NEFA levels should be increased due to defective suppression of lipolysis by insulin. Currently, we do not know the mechanisms by which *Klf14* deficiency in adipocytes impairs lipolysis. But impaired lipolysis in female mice is accompanied by a decrease in *Pnpla2* mRNA and decreased isoproterenol-induced pHSL in adipocytes of both sWAT and pWAT. Decreased pHSL in male *Klf14*-deficient adipocytes alone was not sufficient to decrease lipolysis when *Pnpla2* mRNA was normal. Future studies will establish whether *Pnpla2* is a primary target of KLF14 and whether transcriptional *Pnpla2* regulation is sex specific.

HSL was once thought to be the key enzyme that regulates cellular TG breakdown. Its activity is modulated by phosphorylation (33) However, *Hsl*-deficient mice had a normal rate of free fatty acid production, indicating that other enzymes are playing a key role in TG breakdown (50). Haemmerle et al. (51) identified ATGL as the rate-limiting enzyme in the mobilization of cellular TG. Notably, they reported that mice with inactivated ATGL displayed deleterious metabolic phenotypes similar to those of our female mice with *Klf14*-deficient adipocytes. These include increased adipose tissue mass, decreased insulin sensitivity, impaired energy metabolism, and decreased availability of free fatty acids (51). The latter fostered the use of carbohydrates as the primary fuel despite the presence of increased amounts of fat in the adipose tissue. Reduced TG hydrolysis then led to reduced energy expenditure and total activity. This study supports the notion that defective lipolysis in mice with *Klf14*-deficient adipocytes leads to a switch to carbohydrates as the predominant source of energy, decreased energy expenditure and activity, and increased fat mass gain. The fact that glucose tolerance is not impaired in mice with *Klf14*-deficient adipocytes despite impaired insulin sensitivity may be explained by the energy substrate switch to glucose and decreased cellular NEFA uptake facilitating instead glucose uptake into tissues. The decreased locomotor activity in

female *Klf14*-deficienct mice is possibly attributed to decreased lipolysis and decreased lipid uptake as well, which may mean that they do not have enough nutrients to use as an energy source.

The increased size of parametrial/visceral but normal size of subcutaneous adipocytes in females with adipocyte *Klf14* deficiency could, at least in part, be explained by the more drastically reduced nonstimulated lipolysis in pWAT-derived adipocytes. In addition, other processes, such as increased expression of *Dgat1* in parametrial/visceral adipocytes, may further contribute to increased cell size. Mice that overexpress Dgat1 in adipocytes have increased deposition of TG in WAT (52). Although fatty acid uptake is impaired in adipocytes, as decreased expression of key fatty acid binding/transporter proteins and impaired NEFA clearance suggest, fatty acids taken up could be efficiently esterified to TG due to the increase in *Dgat1*. Increased *Dgat1* expression cannot be explained by increased insulin resistance. In contrast, Dgat1 expression positively correlates with insulin sensitivity in human subjects (53). Specific transcription factors regulating Dgat1 expression have not been identified, but peroxisome proliferator–activated receptor-γ is a candidate (54). Whether KLF14 directly or indirectly controls Dgat1 expression will need to be investigated.

Interestingly, male mice, despite decreased fat mass and smaller adipocytes, did not show improved metabolic parameters and greater insulin sensitivity compared with WT littermates. It is possible that simultaneous changes in fatty acid transporter/binding proteins in the smaller adipocytes are leading to unfavorable changes that are, however, offset by improved insulin sensitivity.

Previous mouse studies showed conflicting results for KLF14 on metabolic phenotypes and atherosclerosis. We recently reviewed these studies (5), several of which only used male mice to study the impact of KLF14 deletion or overexpression, a consequential omission given that in humans and in our study, KLF14 plays sexual-dimorphic roles. Some of the studies also used different diet compositions, which may be another source for conflicting results.

Klf14 adipocyte-specific KO mice have been partially characterized before by Small et al. (1). Similar to our findings, female *Klf14*-deficient mice had decreased HDL-C and impaired insulin sensitivity. However, Small et al. also observed impaired insulin sensitivity in male *Klf14*-deficient mice, contrasting with normal insulin sensitivity in our male mice. Furthermore, glucose tolerance was normal in our *Klf14*-deficient mice, while Small et al. showed defects in both male and female mice. The differences in results could be attributed to several factors. First, different diets were used. Small et al. used a regular chow diet while we fed the mice an HFD. Second, glucose tolerance and insulin tolerance tests were assessed differently. For the glucose tolerance test, Small et al. fasted mice overnight, while we fasted them for 6 h. For the insulin tolerance test, Small et al. used insulin at 1 unit/kg body weight following 4 h of fasting while we used it at 0.75 units/kg body weight without fasting. Our more thorough characterization, including metabolic cage studies and lipolysis assays, then uncovered the clear differences between male and female *Klf14*-deficient mice that we report in here.

Finally, we showed a metabolically favorable consequence of increased expression of adipocyte KLF14: female *Klf14*-OE mice accumulated less body fat in response to the HFD challenge. Although a comprehensive characterization will be required to further flesh out the phenotype of these mice, results from this initial assessment is of therapeutic interest. Previous studies showed that perhexiline, an approved therapeutic small molecule presently in clinical use to treat angina and heart failure, induced KLF14 expression and reduced atherosclerosis (55). Our results, together with the results from this previous pharmacological study, suggest that therapeutic targeting of KLF14, specifically in adipose tissue, could serve as a novel approach to improve metabolic abnormalities in obesity and related metabolic diseases specifically in females.

Acknowledgments. The authors thank the members of the Civelek laboratory for their feedback and discussion, Dr. Stephen B. Abbott (University of Virginia) for assistance in indirect calorimetry analysis, and Dr. Michael M. Scott (University of Virginia) for the assistance in EchoMRI.

Funding. This work was supported by National Institute of Diabetes and Digestive and Kidney Diseases (R01 DK118287 to M.C.) and by the American Diabetes Association (1-19-IBS-105 to M.C.).

Duality of Interest K.M. is an advisor to and holds equity in Verve Therapeutics and Variant Bio. No other potential conflicts of interest relevant to this article were reported.

Author Contributions. Q.Y., S.R.K., and M.C. drafted the article. Q.Y. and M.C. conceived the study, J.H., J.N.R., R.A., and Z.X. participated in data collection and analysis. T.E.H., E.J.S., and S.R.K. contributed to the experimental design and data interpretation. K.M. generated *Klf14*$^{fl/fl}$*Adipoq*-Cre^{+} mice. M.C. directed the study. All authors edited the final article. M.C. is the guarantor of this work and, as such, had full access to all the data in the study and takes responsibility for the integrity of the data and the accuracy of the data analysis.

Prior Presentation. Parts of this study were presented in abstract form at the Don S. Fredrickson Lipid Research Conference, University of Kentucky, Louisville, KY, 9–11 September 2021.

References

1. Small KS, Todorčević M, Civelek M, et al. Regulatory variants at KLF14 influence type 2 diabetes risk via a female-specific effect on adipocyte size and body composition. Nat Genet 2018;50:572–580

2. Teslovich TM, Musunuru K, Smith AV, et al. Biological, clinical and population relevance of 95 loci for blood lipids. Nature 2010;466:707–713

3. Voight BF, Scott LJ, Steinthorsdottir V, et al.; MAGIC investigators; GIANT Consortium. Twelve type 2 diabetes susceptibility loci identified through large-scale association analysis. Nat Genet 2010;42:579–589

4. Chen G, Bentley A, Adeyemo A, et al. Genome-wide association study identifies novel loci association with fasting insulin and insulin resistance in African Americans. Hum Mol Genet 2012;21:4530–4536

5. Yang Q, Civelek M. Transcription Factor KLF14 and metabolic syndrome. Front Cardiovasc Med 2020;7:91
6. Civelek M, Wu Y, Pan C, et al. Genetic regulation of adipose gene expression and cardio-metabolic traits. Am J Hum Genet 2017;100:428–443
7. Civelek M, Lusis AJ. Systems genetics approaches to understand complex traits. Nat Rev Genet 2014;15:34–48
8. Civelek M, Lusis AJ. Conducting the metabolic syndrome orchestra. Nat Genet 2011;43:506–508
9. GTEx Consortium. The Genotype-Tissue Expression (GTEx) project. Nat Genet 2013;45:580–585
10. Small KS, Hedman AK, Grundberg E, et al.; GIANT Consortium; MAGIC Investigators; DIAGRAM Consortium; MuTHER Consortium. Identification of an imprinted master trans regulator at the KLF14 locus related to multiple metabolic phenotypes. Nat Genet 2011;43:561–564
11. Liu DJ, Peloso GM, Yu H, et al.; Charge Diabetes Working Group; EPIC-InterAct Consortium; EPIC-CVD Consortium; GOLD Consortium; VA Million Veteran Program. Exome-wide association study of plasma lipids in >300,000 individuals. Nat Genet 2017;49:1758–1766
12. Willer CJ, Schmidt EM, Sengupta S, et al.; Global Lipids Genetics Consortium. Discovery and refinement of loci associated with lipid levels. Nat Genet 2013;45:1274–1283
13. Jones AS, Johnson MS, Nagy TR. Validation of quantitative magnetic resonance for the determination of body composition of mice. Int J Body Compos Res 2009;7:67–72
14. Fantin VR, Wang Q, Lienhard GE, Keller SR. Mice lacking insulin receptor substrate 4 exhibit mild defects in growth, reproduction, and glucose homeostasis. Am J Physiol Endocrinol Metab 2000;278:E127–E133
15. Wortley KE, del Rincon J-P, Murray JD, et al. Absence of ghrelin protects against early-onset obesity. J Clin Invest 2005;115:3573–3578
16. Fentz J, Kjøbsted R, Birk JB, et al. AMPKα is critical for enhancing skeletal muscle fatty acid utilization during in vivo exercise in mice. FASEB J 2015;29:1725–1738
17. Hargett SR, Walker NN, Hussain SS, Hoehn KL, Keller SR. Deletion of the Rab GAP Tbc1d1 modifies glucose, lipid, and energy homeostasis in mice. Am J Physiol Endocrinol Metab 2015;309:E233–E245
18. Berry R, Church CD, Gericke MT, Jeffery E, Colman L, Rodeheffer MS. Imaging of adipose tissue. Methods Enzymol 2014;537:47–73
19. Schneider CA, Rasband WS, Eliceiri KW. NIH Image to ImageJ: 25 years of image analysis. Nat Methods 2012;9:671–675
20. Parlee SD, Lentz SI, Mori H, MacDougald OA. Quantifying size and number of adipocytes in adipose tissue. Methods Enzymol 2014;537:93–122
21. Fan W, Xu Y, Liu Y, Zhang Z, Lu L, Ding Z. Obesity or overweight, a chronic inflammatory status in male reproductive system, leads to mice and human subfertility. Front Physiol 2018;8:1117
22. Kumar A, Lawrence JC Jr, Jung DY, et al. Fat cell-specific ablation of rictor in mice impairs insulin-regulated fat cell and whole-body glucose and lipid metabolism. Diabetes 2010;59:1397–1406
23. Cirera S. Highly efficient method for isolation of total RNA from adipose tissue. BMC Res Notes 2013;6:472
24. Kwon H, Kim D, Kim JS. Body fat distribution and the risk of incident metabolic syndrome: a longitudinal cohort study. Sci Rep 2017;7:10955
25. Després J-P, Lemieux I, Bergeron J, et al. Abdominal obesity and the metabolic syndrome: contribution to global cardiometabolic risk. Arterioscler Thromb Vasc Biol 2008;28:1039–1049
26. Björntorp P, Sjöström L. Number and size of adipose tissue fat cells in relation to metabolism in human obesity. Metabolism 1971;20:703–713
27. Björntorp P, Grimby G, Sanne H, Sjöström L, Tibblin G, Wilhelmsen L. Adipose tissue fat cell size in relation to metabolism in weight-stabile, physically active men. Horm Metab Res 1972;4:182–186
28. Haller H, Leonhardt W, Hanefeld M, Julius U. Relationship between adipocyte hypertrophy and metabolic disturbances. Endokrinologie 1979;74:63–72
29. Salans LB, Knittle JL, Hirsch J. The role of adipose cell size and adipose tissue insulin sensitivity in the carbohydrate intolerance of human obesity. J Clin Invest 1968;47:153–165
30. Duncan RE, Ahmadian M, Jaworski K, Sarkadi-Nagy E, Sul HS. Regulation of lipolysis in adipocytes. Annu Rev Nutr 2007;27:79–101
31. Fain JN, Garci¬a-Sáinz JA. Adrenergic regulation of adipocyte metabolism. J Lipid Res 1983;24:945–966
32. Morimoto C, Tsujita T, Sumida M, Okuda H. Substrate-dependent lipolysis induced by isoproterenol. Biochem Biophys Res Commun 2000; 274:631–634
33. Watt MJ, Holmes AG, Pinnamaneni SK, et al. Regulation of HSL serine phosphorylation in skeletal muscle and adipose tissue. Am J Physiol Endocrinol Metab 2006;290:E500–E508
34. Ibrahim MM. Subcutaneous and visceral adipose tissue: structural and functional differences. Obes Rev 2010;11:11–18
35. Abumrad N, Harmon C, Ibrahimi A. Membrane transport of long-chain fatty acids: evidence for a facilitated process. J Lipid Res 1998;39: 2309–2318
36. Febbraio M, Hajjar DP, Silverstein RL. CD36: a class B scavenger receptor involved in angiogenesis, atherosclerosis, inflammation, and lipid metabolism. J Clin Invest 2001;108:785–791
37. Abumrad NA, el-Maghrabi MR, Amri EZ, Lopez E, Grimaldi PA. Cloning of a rat adipocyte membrane protein implicated in binding or transport of long-chain fatty acids that is induced during preadipocyte differentiation: homology with human CD36. J Biol Chem 1993;268:17665–17668
38. Haq RU, Christodoulides L, Ketterer B, Shrago E. Characterization and purification of fatty acid-binding protein in rat and human adipose tissue. Biochim Biophys Acta 1982;713:193–198
39. Linn TC, Srere PA. Identification of ATP citrate lyase as a phosphoprotein. J Biol Chem 1979;254:1691–1698
40. Wakil SJ. A malonic acid derivative as an intermediate in fatty acid synthesis. J Am Chem Soc 1958;80:6465–6465
41. Alberts AW, Strauss AW, Hennessy S, Vagelos PR. Regulation of synthesis of hepatic fatty acid synthetase: binding of fatty acid synthetase antibodies to polysomes. Proc Natl Acad Sci U S A 1975;72:3956–3960
42. Cases S, Smith SJ, Zheng YW, et al. Identification of a gene encoding an acyl CoA:diacylglycerol acyltransferase, a key enzyme in triacylglycerol synthesis. Proc Natl Acad Sci U S A 1998;95:13018–13023
43. de Ridder CM, Bruning PF, Zonderland ML, et al. Body fat mass, body fat distribution, and plasma hormones in early puberty in females. J Clin Endocrinol Metab 1990;70:888–893
44. Simmen RCM, Pabona JMP, Velarde MC, Simmons C, Rahal O, Simmen FA. The emerging role of Krüppel-like factors in endocrine-responsive cancers of female reproductive tissues. J Endocrinol 2010;204:223–231
45. Bjørndal B, Burri L, Staalesen V, Skorve J, Berge RK. Different adipose depots: their role in the development of metabolic syndrome and mitochondrial response to hypolipidemic agents. J Obes 2011;2011:490650
46. Gallagher D, Visser M, Sepúlveda D, Pierson RN, Harris T, Heymsfield SB. How useful is body mass index for comparison of body fatness across age, sex, and ethnic groups? Am J Epidemiol 1996;143:228–239
47. Schreiner PJ, Terry JG, Evans GW, Hinson WH, Crouse JR 3rd, Heiss G. Sex-specific associations of magnetic resonance imaging-derived intra-abdominal and subcutaneous fat areas with conventional anthropometric indices: the Atherosclerosis Risk in Communities Study. Am J Epidemiol 1996; 144:335–345
48. Demerath EW, Sun SS, Rogers N, et al. Anatomical patterning of visceral adipose tissue: race, sex, and age variation. Obesity (Silver Spring) 2007;15:2984–2993
49. Chabowski A, Coort SLM, Calles-Escandon J, et al. Insulin stimulates fatty acid transport by regulating expression of FAT/CD36 but not FABPpm. Am J Physiol Endocrinol Metab 2004;287:E781–E789

50. Osuga J, Ishibashi S, Oka T, et al. Targeted disruption of hormone-sensitive lipase results in male sterility and adipocyte hypertrophy, but not in obesity. Proc Natl Acad Sci U S A 2000;97:787–792

51. Haemmerle G, Lass A, Zimmermann R, et al. Defective lipolysis and altered energy metabolism in mice lacking adipose triglyceride lipase. Science 2006;312:734–737

52. Chen HC, Stone SJ, Zhou P, Buhman KK, Farese RV Jr. Dissociation of obesity and impaired glucose disposal in mice overexpressing acyl coenzyme A: diacylglycerol acyltransferase 1 in white adipose tissue. Diabetes 2002;51:3189–3195

53. Ranganathan G, Unal R, Pokrovskaya I, et al. The lipogenic enzymes DGAT1, FAS, and LPL in adipose tissue: effects of obesity, insulin resistance, and TZD treatment. J Lipid Res 2006;47:2444–2450

54. Yen C-LE, Stone SJ, Koliwad S, Harris C, Farese RV Jr. Thematic review series: glycerolipids. DGAT enzymes and triacylglycerol biosynthesis. J Lipid Res 2008;49:2283–2301

55. Guo Y, Fan Y, Zhang J, et al. Perhexiline activates KLF14 and reduces atherosclerosis by modulating ApoA-I production. J Clin Invest 2015;125:3819–3830